Gravel Transport in a Floodplain Wetland Restoration Experiment, Big Spring Run, Lancaster PA

Aakash Ahamed
Earth and Environment Department
Franklin and Marshall College

Advisor: Candace A. Grand Pre, Department of Earth and Environment
Franklin and Marshall College
ENV 490: Independent Study
Project Submission: April 30th, 2012
Graduation: May 12th, 2012

Honors Thesis Defense Committee:
Dorothy Merritts, Earth and Environment, Franklin and Marshall College
Suzanna Richter, Earth and Environment, Franklin and Marshall College
Drew Altland, Cardno ENTRIX

Table of Contents

1. Abstract

A headwater reach of Big Spring Run (BSR), PA, a low-relief 2nd-order Piedmont stream (drainage area 15 km^2) in the Chesapeake Bay watershed, is the site of an ongoing investigation to test a relatively new stream restoration approach. This study examined bedload entrainment and calculates critical shear stresses for intermediate to high stage conditions at BSR before restoration, which was completed between August and November 2011. A USGS gage station at the downstream end of the restoration reach recorded stream discharge to be between a base flow of 0.1 cubic meters/second (cms) and ~6 cms from September 2009 to July 2011. In the restoration reach I recorded bedload transport of painted tracer gravel occurred during moderate to large flow events at basal shear stresses of 54–110 Pa for water depths of 0.8–1.6 m. Prior to restoration, the BSR channel frequently transported a bedload of gravel-sized clasts. Since restoration, water depth has been substantially decreased and water-surface slope has been slightly decreased. Restoration work removed 21,000 m^3 of historic sediment, significantly lowering water depth for the bankfull condition and establishing small anastomosing stream channels similar to the pre-European settlement wet meadow environment. One of the major implications of the restoration project is that basal shear stresses will be dramatically reduced to less than <1.5 Pa for water depths up to 0.2 m. This study predicts that under these reduced shear stress conditions the post-restoration reach of BSR will be able to transport sediment no larger than 10 mm in diameter, which is ~500% smaller than the grain size mobilized before restoration. Future post-restoration monitoring of gravel mobility will test our predictions of decreased shear stress due to the restoration.

2. Introduction

Recent research conducted throughout the Chesapeake Bay watershed demonstrates that many modern stream channels and banks of the mid-Atlantic region are anthropogenic in origin (Walter and Merritts, 2008). Modern gravel-bedded sinuous channels are incised into thick accumulations of massive sand silt and clay, which overlie a basal hydric soil. Merritts et al. (2011) describe this morphology as a result of human modifications that began with damming valleys in the late 17th century. Widespread dam building led to historic sedimentation along valley bottoms. Figure 1 shows the number of dams that have been identified in York, Lancaster, and Chester Counties, Pennsylvania. In each county ~400 dams have been recognized, all which have caused significant and pervasive sedimentation. The implications of the discovery of the human origins of legacy sediments in Walter and Merritts (2008) and Merritts et al. (2011) include 1) a reconsideration of the initiation of bedload and evolution of meandering streams in the northeastern United States; and 2) the need to reconsider the natural baseline environmental conditions to be used as a restoration target (Montgomery, 2008). Restoration was completed on one of these anthropogenic streams, Big Spring Run, Pennsylvania, in an effort to convert a single deeply-incised channel into a freshwater wetland with small branching stream channels, which is similar to the condition of the pre-settlement environment that characterized this region before the 17th century (Merritts et al., 2011).

Restoration efforts in this region are critical to the health of the Chesapeake Bay, an impaired water body under the Clean Water Act and the largest estuary in the United States (Phillips, 2002). The Chesapeake Bay drainage basin covers 165,759 km^2 (Senus et al., 2005). In 2003, the USGS estimated that 18,200 million pounds of sediment, including 350 million pounds of nitrogen and 30 million pounds of phosphorous was deposited into the Chesapeake, having a devastating effect on fisheries and the health of the estuary (Langland et al, 2005). Erosion of historic sediment exposed along incised stream banks is one of the primary sources of this fine-grained sediment to the Bay (Merritts et al, 2011).

In order to reduce suspended sediment loads to the Bay, a restoration method is needed that will reduce erosion of channel banks and reduce sediment transport into the Chesapeake.

Shilling (2010) estimates that lateral bank retreat rates at BSR are 23.9 centimeters/year (cm/yr) for type 1a banks (height = 1.1 m) and 31.1 cm/yr for type 1b banks (height = 0.9 m), yielding annual sediment loads as high as 151 tons per year from the restoration reach of BSR. BSR is listed on the United States Environmental Protection Agency's Clean Water Act section 303(d) list of degraded water bodies due to its high loads of suspended sediments and nutrients (EPA). The EPA's 303(d) classification of this stream and the ongoing geomorphic research conducted at BSR since the 1990s made it a prime candidate for a steam restoration experiment with pre- and post-restoration monitoring.

In this paper, I assess the transport of gravel-sized clasts in an incised anthropogenic stream channel by studying active bedload sediment transport at BSR during storms. It is one of the first studies in the mid-Atlantic northeast United States in which the anthropogenic nature of the stream is considered when empirically evaluating gravel transport and the implications of restoration. The abundance of wet meadow seeds in the dark hydric soil buried beneath the blanket of historic sediment indicates that Big Spring Run was a wet meadow environment prior to being buried by fine sands, silts and clays (Merritts and Walter, 2011). The deeply incised banks of the pre-restoration stream channel allowed for higher water depths during high flow events, causing a substantial increase in shear stress acting on entrained particles in the streambed (Wiberg and Smith, 1987). Therefore, stream competence and stream capacity also were increased, and the altered stream was capable of transporting much larger particles than its wet meadow predecessor (Walter and Merritts, 2008, Voli et al, 2009, Hilgartner et al, 2010). Clasts below the pre-Holocene wetland soil are cobble to boulder in size (Merritts et al., 2011), and prior to restoration, clasts as large as cobbles were frequently moved by high flow events. The ability of BSR to transport large gravel clasts on an armored bed has significant implications for its potential to transport smaller silts and clays that make up the banks. Concordantly, if channel height is reduced significantly, stream competence and capacity will decrease, reducing the rate of erosion and transport of the fine sediments that eventually enter the Chesapeake. This sediment will be trapped in place, unable to be transported.

I measured the size of clasts transported during storms at Big Spring Run from 2008 to 2012. Based on the data I collected, I estimate the potential carrying capacity and maximum clast-size that will be transported at BSR and other anthropogenically impacted streams after restoration. These estimates will be compared with measurements of actual gravel transport after restoration.

3. Study Area

BSR is a low-relief (slope = 0.05 to 0.07 m/m), 2nd-order (15 km^2) Piedmont stream located in southeastern Pennsylvania within the Chesapeake Bay watershed (Figures 2 and 3). It is an anthropogenic stream, owing its current morphology to the construction and subsequent breaching of dammed mill-ponds erected in Pennsylvania in the 17th through late 19th centuries (Walter and Merritts, 2008). The bedrock consists of weathered Paleozoic limestone with thick quartz veins (Merritts et al., 2011). The limestone is mapped on the Quarryville and Conestoga quadrangles as Cambrian to Ordovician age Conestoga formation, which consists of light to medium gray crystalline limestone with phyllitic partings and medium gray phyllitic limestone (Blackmer, 2007). BSR lies within the Lancaster belt, a structurally complex area that has undergone repeated cycles of deformation, faulting, and isoclinal folding (Galeone et al., 2006). Overlying the bedrock is a 0.1 to 0.3 m thick layer of angular to sub-angular gravel and cobble-sized clasts, presumed to be pre-Holocene periglacial sediment, which formed aprons along toe of slope areas. (Merritts et al., 2011). A 0.1 to 0.6 m thick hydric organic-rich soil overlies the Pleistocene colluvium in most places, lapping onto toes of aprons along valley bottom margins. Atop the hydric soil rests ~1 – 1.2 m of fine (95% silt and clay content) and cohesive, light brown sediment (Merritts et al., 2011).

Periglacial landscapes, which included BSR, have experienced considerable environmental change since the Last Glacial Maximum (LGM) (Merritts et al., 2011). BSR is located ~100 km south of the LGM Laurentide Ice Sheet terminus (Merritts et al., 2011). This Appalachian region experienced a high degree of mechanical weathering and denudation during the end of the Pleistocene (Montgomery and Wohl, 2003). Periglacial processes including gelifluction, solifluction, and creep delivered angular gravel (pebble-boulder size) to valley bottoms (Merritts, unpublished data). These periglacially transported clasts manifest as lobes of gravel deposited in toes-of-slope areas (Merritts et al., 2011). Following the LGM, climate began to warm to interglacial conditions. The Laurentide ice sheet melted and retreated. The environment changed from periglacial to a warmer and more temperate environment. Wetlands began to form in abundance in the valley bottoms and accumulated peat throughout the Holocene (Merritts et al., 2011). A modern analog to BSR during the LGM is the valley bottoms found in current periglacial landscapes in Alaska (Figure 4).

The streambanks at BSR are consistent with the regional stratigraphy, containing 3 distinct stratigraphic units (Figures 5 and 6). The bottom most layer, which is 0.1 – 0.3 m in thickness is composed of a quartz rich gravelly substrate that Merritts et al. (2011) propose was transported downslope as colluvium by mass wasting processes such as gelifluction and solifluction. The second layer is a dark, organic rich, hydric soil that is 0.1 - 0.6 m in thickness. This hydric soil contains seeds, nuts, wood, and other organic matter interpreted to represent a pre-European settlement freshwater wetland (Neugebauer et al. 2011). The overlying layer, known as “Legacy Sediment”, is comprised of a light brown, extremely fine (95% fine sand, silt and clay), cohesive clastic sediment that was deposited after post-colonial dams flooded the valley bottoms and allowed these fine sediment to settle out of suspension (Merritts et al, 2011).

Extensive macrofossil analysis on preserved seeds and plant fragments indicate that this buried soil formed in a water-logged freshwater environment (Neugebauer et al, 2011). Plant assemblages are dominated by *Carex* spp. taxa common to modern freshwater wet meadow environments. 2,485 seeds and additional organic materials were sampled from this laterally-extensive buried soil. Radiocarbon ages derived from seeds estimate the maximum age of the soil at this location to be 3,300 - 3,000 cal. yrs. BP at the bottom of the layer, and ~ 300 cal. Yrs. BP at the top. Overlying the paleo-wetland soil is a ~1 m deposit of laterally continuous massive fine sands, silts and clays. Due to dam building and subsequent breaching, Walter and Merritts (2008) interpret the BSR site to have evolved from a wet-meadow with anabranching channels to an incised single-thread meandering channel. Before restoration in August, 2011, the channel was incised into ~1.1 meters of fine-grained sediment.

4. Methods

4.1 Tracer Gravel

Using tracer gravel particles is an inexpensive and effective way to evaluate gravel transport (Hassan and Ergenzinger, 2003). In June, 2010, following the methods of Fraley et al., (2006), I collected 25 quartz clasts (density = 2.65 g/cm^3), which were representative of the approximate gravel size from the active bed of BSR. After collection I painted the clasts fluorescent orange to make them easier to spot. I ranked and labeled the 25 clasts in relative size based on the cumulative lengths of their A, B, and C axes, with #1 being the smallest and #25 the largest. The spray-painted and numbered clasts were placed on the streambed at two sites (Figure 2) deemed to be conducive to gravel transport due to their relatively deep water and steep channel gradient. The two sets of tracer gravel were similar in size.

Following the methods of Snyder et al., (2008) I placed the painted clasts into a circular area with a diameter of ca. 0.5 m. Survey flags were placed on the banks and in the bed to mark the original position of the gravel. After several high-flow events, I modified the experiment in order to measure transport distance more precisely. By changing our methodology, I sought to obtain more specific and accurate measurements of direction and distance transported. Data obtained using the initial methodology was preserved and has been utilized in this study. In order to better track the original locations in the streambed I designed and constructed a wooden grid to be used for the duration of the experiment from June 16, 2010 to March 6, 2011 (Figure 7). I placed the gravel clasts 7 cm apart from each other in the wooden grid, positioned so that the smallest clasts were upstream and the largest downstream A flag was placed in the streambed to mark the middle point of the grid.

After each moderate to high storm flow event, I recovered the orange clasts and measured the distance and direction the clast traveled during the storm. The clasts were then collected and returned to their original positions within the wooden grid. Some clasts (<25%) were not recovered due to burial or inability to locate the clast.

On March 6, 2011, I introduced a new methodology following Snyder et al., (2008). This methodology involved placing gravel clasts in a row across the streambed, perpendicular to the thalweg of the channel. I positioned a camera and stadia rod at the site of the orange clasts to photo-document bank erosion and water height during high-flow events. After each of the 13 high-flow storms I located the new positions of the orange clasts and recorded their distance and direction of transport. I then removed the clasts from the stream and placed them in the starting position to repeat the experiment.

4.2 Particle Size Analysis

I collected sediment samples from seven depositional sites along BSR's active channel (Figure 3) using a shovel and bucket. Approximately 1 kg of each sample was collected from a 0.25 x 0.25 m quadrant. I conducted a full grain size distribution using Wentworth scale sieves following the methods of Gee et al., (1986) and cumulative percentages were calculated following the methods of Gee et al., (1986). The D_{50} and D_{84} were determined in order to gain additional insight about gravel bar formation and gravel transport during high flow events.

On June 11, 2010 I collected three samples from the cut-bank of a point bar (Figure 3). I labeled the samples “Gravel Bar 1”, “Gravel Bar 2”, and “Point Bar”. Historic air photos reveal that the gravel point bars at this location began to form in the 1950s after channel incision had occurred. The channel migrated westward by erosion of the left (western) bank between 1950 and 2010. The point bar on right bank formed in the wake of the retreating bank. The meander bend also shifted downstream, so that the upstream end of the point bar began to erode. This erosion produced a fresh exposure that I used for sampling the entire depositional sequence of bar from bottom to top. I collected these samples in order to have a representative distribution of particle sizes in a point bar. The sediment in a point bar is that which was transported from upstream during recent flow events, so the point bar contains an archival record of bedload sediment transport.

I collected three additional samples following a high flow event on June 16th 2010. During this storm water depth reached 1.6 m, which is roughly bankfull stage. Two of the three samples, labeled “Overbank Flood Deposit 6/16/10” and “Point Bar Flood Deposit 6/16/10” in Figure 3, were collected from a small crevice splay (~1m) of gravel that breached the channel cutbank and splayed on to the floodplain. Some smaller pieces of gravel were transported over the bank farther along the floodplain, forming an elongate lobe of gravel that was deposited on the planar surface adjacent to the incised stream. This sample was labeled the “Overbank Flood Deposit”.

Grain size was measured using 0.297 mm, 2 mm, 3.35 mm, 5 mm, 12.7 mm, and 13.3 mm sieves. Grain size analysis and cumulative percent analysis were conducted following the methods of Gee et al., (1986).

4.3 Calculations: Shear Stress and Shields Parameter

Critical shear stress is defined as the amount of parallel force applied perpendicular to normal force required for initialization of motion of a particle (Leopold et al, 1964). Shields parameter is a dimensionless number related to shear stress used to calculate the initiation of motion of sediment in a fluid flow (Shields, 1936). Snyder et al. (2010), Reitz et al. (2011), Jerolmack et al. (2011), and Wiberg and Smith (1987) demonstrated that shear stress and the Shields Parameter can be used to assess stream competence. I calculated shear stress for our samples using the formula:

$$\tau_b = \rho g h S$$

where τ_b = shear stress (Pa), ρ = density of water (assumed to be 1000 g/m^3), g = acceleration due to gravity (9.8m/s^2), h = water depth (m), and s = slope (m/m).

I calculated critical shear stresses using the related variables of water depth and hydraulic radius (R=A/P), where R=hydraulic radius, A=cross sectional area of the channel, and P=wetted perimeter (Buffington and Montgomery, 1997). Hydraulic radius was attained in order to characterize shear stresses associated with bankfull and overbank flows.

Both water depth and wetted perimeter were employed in order to obtain shear stresses and Shields parameters. Therefore, the two data sets obtained using depth and hydraulic radius are both related to average depth of the channel. Hydraulic radius is calculated by dividing cross sectional area of the channel by wetted perimeter. Being that the hydraulic radius increases as channel depth increases, while wetted perimeter remains relatively constant at the study site, these parameters are closely related.

I calculated the channel bed slope to be 0.007 m/m by measuring the difference in elevation between two locations close to the study site where bedrock was exposed in the streambed. I also measured the difference in water surface elevation between two points using LIDAR data (NCALM LIDAR, flown October, 2008) and confirmed the slope to be 0.007 m/m. Water depth, in meters, was derived from a USGS gauge station located close to the study site at Lat 39\`59'45.37", long 76\`15'50.54”.

Shields Parameter was calculated using the formula:

$$\tau * = \frac{\tau}{(\rho_s - \rho)(g)(D)}$$

where τ_* = Shields parameter, τ = Shear stress, ρ_s = Density of sediment (assumed to be 2650 g/m^3), ρ = density of water (assumed to be 1000 g/m^3), g = acceleration due to gravity (9.8m/s^2), and D = particle diameter (D_{50} of b-axis of transported clasts) (Buffington and Montgomery, 1997). The result yields a dimensionless (unitless) number.

I calculated the boundary Reynolds number (Buffington and Montgomery, 1997) with the following equation:

$$\mathrm{Re} = \frac{\rho \mathrm{v} L}{\mu} = \frac{\mathrm{v} L}{\nu}$$ [

where v = mean velocity of the object relative to the fluid (m/s), •L = hydraulic diameter (m), •μ = dynamic viscosity of the fluid (Pa·s or N·s/m² or kg/(m·s)), •*v* = the kinematic viscosity (m²/s), and •*ρ* = density of the fluid (kg/m³). The boundary Reynolds number was used to account for the influence of inertial and viscous forces on the results (Snyder et al., 2008).

4.4 Wolman Pebble Count

In order to measure the range and variation in grain size of the bed, I conducted a Wolman pebble count at the "type locality". The a, b, and c axes of 100 randomly selected clasts were measured along a 3 m by 3 m section of the bed (Leopold et al.,1964).

5. Results

5.1 Shear Stress and Shields Parameter

Table 1 shows the results for samples collected following 13 storms from June 16th, 2010 to April 28th, 2011. The most intense storm occurred on July 26th 2010, and the water reached a bankfull depth of 1.6 m. Using this water depth (h), I calculated shear stress to be 109.76 Pa and the Shields parameter to be 0.09 (dimensionless number). By substituting water depth (h) with hydraulic radius (R) the shear stress becomes 45.86 Pa. The D_{50} of clasts transported at least 30 cm was 33.12 mm.

The least intense storm recorded occurred on June 24th, 2010, reaching a water depth of 0.79 m. Using this water depth (h), I calculated shear stresses to be 53.97 and the Shields parameter to be 0.09. By substituting water depth (h) with hydraulic radius (R) the shear stress becomes 32.33 Pa. The D_{50} of clasts transported over 30 cm was 23.35 mm.

A storm that reflects the average water depth for the 13 storms recorded occurred on April 5th, 2011, reaching a water depth of 0.88 m. Using this water depth (h), I calculated shear stress to be 60.43 Pa and a Shields parameter of 0.05. By substituting water depth (h) with hydraulic radius (R) the shear stress becomes 32.15 Pa. The D_{50} of clasts transported over 30 cm was 38.58 mm.

The largest transported clast on record had a b-axis of 66 mm. This clast was moved during the March 11th, 2011 storm, which yielded a shear stress (based on water depth) of 76.32 Pa. The largest calculated shear stress on record is 109.76 Pa (based on water depth), which occurred during the July 26th, 2010 storm. The water depth during this storm reached a height of 1.6 meters and transported clasts with a D_{50} of 33.12 mm. The largest particle transported during this storm had a b-axis of 51.98 mm, and was transported 32 cm.

Shields Parameter for all recorded events ranged from 0.03 - 0.16. The greatest value for the Shields Parameter occurred on June 17th 2010, when water depth reached 0.83 m. Shear Stress vs. D_{50} plots were constructed for thresholds of what could be perceived "initial motion" (see Appendix 1 for more information).

5.2 Particle Size Distribution

I calculated cumulative percentages of the particle size distributions of samples collected from various locations in the BSR restoration reach (Figure 8). The "Historic Fill" sample is composed predominantly of fine sands, silts and clays that built up behind the downstream dam and blanketed the valley bottom following dam breaching. This sample was the finest, followed by "Gravel Bar 1" and "Gravel Bar 2". These samples contained the most silt and clay (<0.297mm fraction) because they were sampled directly from the bank of a point bar, whereas other samples consisted of gravel clasts which were deposited during high flow events. The “Overbank flood deposit”, “Flood Deposit”, “Point Bar Flood Deposit” samples were deposited during the high flow event that occurred June 16th 2010 (water depth = 1.6 m). It is important to note how coarse the “type locality” sample is, as it is composed of extremely coarse periglacial material that becomes bedload when exhumed by bank erosion. The sample is almost entirely coarser than 12.7 mm. Most other samples are between these two extremes, although the “flood deposit” samples had a notably smaller content of fine particles.

6. Discussion

6.1 Tracer Gravel

The primary goal of this ongoing study is to quantify the critical shear stresses associated with gravel transport during high-flow storm events at BSR. Theoretical and calculated data area meant to take a back seat to our empirical findings pertaining to the size of transported particles during high flow events. All data points in this study refer to actual clasts that have been transported. Our data indicate that the particles transported by this small, relatively low gradient stream prior to restoration are a considerable size (largest D_{50} = 52 cm). Grain size analysis of banks and point bars indicates that point bars were composed of much finer material and that the influx of gravel transport is a relatively recent phenomenon. The gravel on the bed of BSR is often misperceived as being fluvial in origin (Leopold and Wolman, 1956). It is unlikely that low gradient, anastomosing pre-settlement wetlands predating BSR were capable of transporting course gravel clasts because lower bank heights result in diminished shear stresses.

The data indicate that water depths of <0.85 m typically transport clasts with a D_{50} below 30 mm (Table 1) while water depths > 1.0 m typically transport clasts with a D_{50} over 30 mm. There is quite a degree of variability associated with the D_{50} of clasts transported during flows between 0.85 m – 1.0 m (D_{50} = 14.63 – 38.58 mm). Low flows (~0.2 m) were not capable of transporting even the smallest pieces of tracer gravel (D = 13 – 15 mm) placed in the streambed. The post-restoration bankfull depth will not exceed 0.2 m, as water will spill over a series of small, anastomosing channels and across a wide floodplain.

The independent variables of depth (h) and hydraulic radius (R) were both used in calculating shear stress in this study. Hydraulic radius (R=A/P), where R=hydraulic radius, A=cross sectional area of the channel, and P=wetted perimeter, was included in the study to characterize the ability of BSR to transport gravel at bankfull and overbank flow. Hydraulic radius is highest at bankfull flows, but decreases during overbank flow. This occurs because when a flow exceeds bank height, wetted perimeter increases rapidly while cross sectional area barely increases at all, yielding a low hydraulic radius value (Figure 9).

My data indicate that particles ranging in size from <1 to 4.85 cm are moved at a water depth of ~0.8-0.9 m. The July 12th, 2010 event had a water height of 0.8 meters, and the largest clast transported was transported only 9.8 cm, and had a B-axis of only 14.6 mm. In contrast, the event that occurred on April 8th, 2011 had a water height of 0.864 meters, and the largest clast transported a significant distance had a B-axis of 48.5 mm. This indicates that an increase in water depth of 0.068 meters, or 7.8%, resulted in the transport of a grain with a B-axis 33.9 mm larger, or 3.32 times greater than the grain that was transported at the 0.8 water depth. The movement of a range of gravel sizes at this minimum water depth suggests a threshold; *i.e.,* at water depths >0.8 m multiple size clasts can be transported.

These results suggest a bi-modal distribution of transport. For greater water depths, I find a general positive correlation, with greater depths associated with larger clasts. The largest flow event was associated with a peak water depth of 1.6 m, and the largest clast moved had a b-axis diameter of 52 mm. However, the largest clast moved during the study period was 56 mm in b-axis dimension, but peak water depth was only 1.1 m.

Furthermore, water-surface slope changes locally for each storm event. In order to characterize shear stresses and shields parameters with a greater degree of precision and accuracy, the slope for each storm event must be determined in addition to water depths.

A problem with the tracer gravel experiment arose when particularly intense storms transported all the gravel. This made it not possible to quantify the maximum competence of the stream during these events. I added larger clasts of tracer gravel to the experiment after such events, but I am unable to determine maximum size class transported for events for which all clasts were moved. This affects the results because the largest clasts capable of being transported during some storms were not recorded. Therefore, the results for average shear stresses are slightly lower than they would have been if larger tracer clasts were present during these events.

Furthermore, gravel clast geometry appears to be an important factor in determining transport. Tracer gravel clast #19 has dimensions of 82.68 mm, 58.19 mm, and 36.05 mm for a, b, and c axes. Tracer gravel clast #20 has dimensions of 105.44 mm, 66.08 mm, and 30.05 mm for a, b, and c axes. Tracer gravel clast #19 was transported more frequently and moved greater distances than tracer gravel clast #20. This could be due to clast geometry. Tracer clast #19 is a rounded, smooth piece of quartz, whereas tracer clast #20 is jagged, angular, and oblong quartz. From repeatedly observing gravel transport after high flow events, it appears that clasts with geometric characteristics similar to tracer clast #19 are more easily transported than clasts with geometric characteristics similar to tracer clast #20. This could be due to the fact that a larger face of clast #19 was exposed to the current, increasing the amount of force per unit area (shear stress) acting on the clast, and thereby transporting it more easily.

Although three different methodologies were employed in the tracer particle study, a compilation of all results obtained from the study have an R^2 value of 0.31 (Figure 10). The focal point of the study was initiation of motion due to forces acting on gravel particles during flood events. The amount or direction of motion, while notable, was not the core goal of our approach. Each method had varying degrees of success at evaluating the magnitude and direction of transport, but I believe that all methodologies effectively captured “incipient motion”. While the gravel grid apparatus yielded much more precise and accurate results for the magnitude and direction of motion, it was equally as effective as the other methods at determining the “initiation of motion” of a particle.

Despite low R^2 values associated with tracer gravel data that plots shear stress against D_{50} and D_{84} (R^2 = 0.21 - 0.35), there still appears to be a causal relationship between water height and particle transport. Further, my results are comparable to a similar published study; Snyder et al (2008) attained R^2 values of 0.199 to 0.355 of mobility against shear stresses/Shields parameters. Furthermore, low R^2 values could be due to small sample size (Parker, 1978), as well as the stochastic nature of river systems (Jerolmack, 2011). In order to gain additional insight about gravel transport during high flow events, a larger number of study sites, as well as a larger number of storms should be incorporated into the results of the study.

Although shear stresses were extremely variable throughout the study (53.97 Pa – 109.76 Pa) the Shields parameters obtained using the D_{50} of mobilized particles fall precisely within the range of transport when plotted on a Shields curve (Figure 11). This indicates that despite variability, the results are meaningful. In the 1 year 4 month study period, significant transport events took place, however the erosive power of a 50-year or 100-year flood remains unknown.

6.2 Particle Size Analysis

Our study involved particle size analyses in order to analyze and better understand the deposition of gravel at certain locations after high flow events. Samples from sites labeled as “Gravel Bar 1”, “Gravel Bar 2”, and “Historic Fill” were collected in order to evaluate the evolution of point bars at this site. The samples were collected from left to right on the bank, so “Gravel Bar 1” was deposited the most recently and “Historic Fill” was deposited before the other samples. This was done in an attempt to chronicle and evaluate the evolution of the point bar. Performing particle size analysis on these samples provides insight as to how they were deposited.

Figure 12 shows a cross section of the point bar from which these samples were taken. A topographic low point occurs on the right of the figure. This is a high-flow channel that also marks the boundary between the gravel bar and the original bank of the incised channel. This explains the disparity in grain size in the Gravel Bar samples, as “Historic Fill” was sampled from the bank of the original channel, which may explain its fine grained composition. “Gravel Bar 2”, on the other hand, is the coarsest sample of the three. Localized backwater also plays a role in the transport and deposition of gravel clasts, and may have influenced the variability in grain size. It is also possible that the differences between Gravel Bar 1 and 2 is just the inherent variability in grain size found in any bar. More sampling in order to measure this inherent variability is necessary to test this hypothesis.

Furthermore, the “Overbank Flood Deposit 6/16/10”, “Flood Deposit 6/16/10”, and “Point Bar Flood Deposit 6/16/10 samples were all deposited following the high flow event that occurred on June 16th 2010 (water depth = 1.6 m). This explains their coarse grain size, as high shear stresses associated with this high flow event transported and deposited larger clasts than a typical event. The “Flood Deposit” sample was formed as a result of a sharp meander bend that sharply decreased slope and therefore limited transport. Due to this, large clasts were scoured and transported at the straight stretch before being deposited when the slope sharply diminished as the channel veered to the east. The decreased slope significantly decreased shear stresses, and the channel deposited these clasts in a ramp-like structure when the channel ran into this sharp meander bend. This ramp structure increased the base level of the stream, and led to a significant number of particles being deposited over the bank due to bankfull flow.

I sampled these overbank deposits, and called them the “Overbank Flood Deposit” sample. Of these samples, the “Point Bar” just around the meander bend was the coarsest, followed by the “Flood Deposit” and “Overbank Flood

Deposit" respectively. This is logical in that only smaller clasts could be transported up and over the bank after the ramp formed. The "Flood Deposit" and the "Point Bar" have a similar percentage of clasts size upwards of 12.7 mm, but the "Point Bar" samples proves to have fewer than 20% of its clasts being finer than 5 mm. These finer clasts may have been washed out of the sample during the high flow event. The bulk of the "Point Bar" sample is composed of clasts between 5 mm and 12.7 mm. This indicates that the stream had the competence to carry large, but not the largest clasts around the sharp meander bend. It is likely that the largest clasts were deposited at the bottom of the ramp underwater, and as a result, were not contained within the "Ramp" sample.

The Wolman pebble count was included in particle size analysis. Measuring the a-, b-, and c- axes of each pebble allowed us to obtain their individual volumes. Using the representative b- axis of each pebble, I ascribed them into the same grain size categories. Volume was multiplied by density to calculate mass for each particle, which allows me to show the cumulative percentages of grain sizes using the pebble count.

In order to gain more precise and accurate data about the movement of gravel at BSR, more sample sites should have been included in this study. Fresh gravel deposited after each high flow event could be sampled and compared with tracer gravel data in order to compare results and gain a better understanding of which sized clasts moved during the storm. Additionally, more gravel and point bars could be sampled in order to characterize what was being moved during earlier high flow events. With more sample sites, the full range of variability at BSR could be determined.

6.3 Implications for Stream Restoration

This research has broad implications for stream restoration within the Chesapeake Bay Watershed. BSR is one of countless anthropogenically impacted, highly incised channels within the greater Chesapeake Bay Watershed. Streams like BSR transport large amounts of fine-grained sediment that eventually leads to the environmental problem of Eutrophication (Smith et al. 1999).

Electrostatic charges associated with clay-sized particles attract oppositely charged phosphates. Nitrates in solution and electrostatically bonded phosphates enter streams as a result of runoff from neighboring farmland. After attaching themselves to clay-sized particles, these nutrients that promote plant growth and productivity are also transported through the watershed until they eventually reach the Chesapeake Bay. Once they do, huge algal blooms form as a result of the influx of nutrients. When these algae die, they sink to the bottom and are decomposed by bacteria. Bacteria use oxygen to decompose the algae, and when the massive algal blooms die, bacteria utilize all available oxygen to decompose them. This creates anoxic dead zones in the bay, devoid of fish or other wildlife. The same problem is present on a greater scale at the Mississippi River Delta. This process is called eutrophication.

Restoring streams impacted by historic sedimentation and channel incision to their former wetland environments can mitigate the erosion of clay and all larger particles, substantially reduce the maximum potential shear stress during flooding events, as well as sequester nitrate, phosphate, ammonium and other forms of nitrogen and phosphorous. Figure 13 is a schematic that depicts the differences between pre- and post-restoration streams. The depths of the banks are greatly reduced, which reduces shear stress and the maximum size of particles that can be transported. Further, the increase in wetland vegetation increases the ability for the wetland to sequester large amounts of nitrate and phosphate and trap fine sediments. Therefore, restoration has great potential to alleviate eutrophication and sediment transport into the Chesapeake Bay and beyond.

Walter and Merritts, (2008) and Leopold and Wolman (1956) emphasize the differences between eastern and western streams and their resulting effects on landscapes and ecosystems. Look no further than the pervasive problem of anoxic dead zones in the Mississippi River Delta and the Chesapeake created as a result of eutrophication. Additionally, the habitats of Atlantic Salmon and other wildlife are being put at risk due to damming and sediment loading (Snyder et al., 2008). The cumulative erosive power of mid-Atlantic, southeast and Midwest watersheds are unique to the region, and therefore must be evaluated bearing in mind the evolution of mid-Atlantic streams in the last 400 years.

Incised channels like that of BSR are prevalent throughout the eastern US. The study of this stream has significant implications when extrapolated to a larger scale. It is likely that many, if not most streams in the mid-Atlantic piedmont are anthropogenic relics and, like BSR, have been altered by centuries of damming. Given the significantly increased erosive power of BSR and the frequency of similar streams on the east coast, the cumulative erosive power of eastern streams could be much higher than previously thought.

The transport of large clasts is a key proxy for overall sediment transport. In many ways, it determines the limitations of the macro-scale geomorphic system (Parker, 1978). Grains traveling by saltation dislodge and weaken other flocculate grains. Wiberg and Smith (1987) state that “Observations of beds composed of a mixture of grain sizes, however, indicate that the coarser material can move at a similar, or even lower, boundary shear stress than is required to move the finer material on the bed”. Angular gravel clasts present on the streambed trap fine sediment. When gravel clasts are dislodged, so is fine sediment that has settled near the top of the bed. Therefore, decreasing stream competence and limiting the transport of large clasts is a key parameter in mitigating the transport of fine sediment that contributes to eutrophication. While gravel transport is not directly linked to the problems of sediment loading, eutrophication, and destruction of ecological habitats in the Chesapeake Bay, it has the potential to serve as an excellent proxy of a stream’s cumulative erosive power.

Wetland restorations recently have gained momentum as viable way to alleviate eutrophication and other environmental problems (Merritts et al., 2011). However, long term monitoring after restoration is uncommon, and the degree of success that they have achieved has not been evaluated fully (Bernhardt et al., 2005). Moving forward, it is crucial to evaluate geophysical parameters like water height, shear stress, and particle transport both before and after restoration in order to establish a framework for what can be defined as a “successful” restoration.

Following restoration, the same criteria will be tested using the aforementioned methodologies. Pre- and post-restoration comparisons between shear stresses, Shields parameters, grain size of recent deposits, and Reynolds numbers will be compared. I predict typical post-restoration shear stresses to be <1.5 Pa for water depths of 0.1 m. At these shear stresses, gravel transport will be limited significantly. During storms, water will spill out over a wide, multi channel floodplain, maintaining low water heights and limiting gravel and sediment transport (Figure 13). Additionally, armored gravel not being transported as bedload has the potential to trap significant amounts of fine sediment, slowing transport and mitigating sediment loading into the Chesapeake.

7. Conclusions

Despite variability among empirical results, there is undeniably a considerable effect of legacy sediment rich streams on sediment transport. Before restoration, Big Spring Run was capable of carrying 7 cm gravel clasts, despite a gentle gradient. Empirical results obtained from tracer gravel studies and grain size analysis, as well as calculated theoretical values indicate that large bank heights substantially increases the erosive power of the stream, reaching shear stresses of over 100 and transporting clasts with a B-axis of over 60mm.

The wetland restoration will almost certainly reduce sediment and gravel transport at BSR. Using Formula 1, I predict shear stress values of <1.5 Pa during flow events of water heights 0.1 m. In turn, eutrophication and sediment loading into standing bodies of water are likely to be mitigated. After the damming of valley bottoms has altered landscapes and ecosystems, it is up to scientists and engineers to design streams that contribute positively to the environment. Big Spring Run could serve as a potential benchmark for wetland and stream restoration.

Stream restoration and the demobilization of gravel have a number of positive effects to the Chesapeake Bay including 1) limiting gravel transport and creation of a basal sediment trap for fine particles; 2) decreasing the capacity and competence of streams thereby mitigating transport of fine sediment; 3) returning the environment toward pre-settlement conditions, which aids in sequestering phosphorus and nitrogen, as well providing a home for numerous endangered and threatened species endemic to this wetland environment; and 4) alleviation of eutrophication and other problems in the Chesapeake Bay watershed. BSR has been the subject of study for more scientists and agencies than any other restoration site. If restoration is successful, BSR could serve as a benchmark for the essential parameters to test before and after restoration in order to ensure success.

8. Acknowledgements

I would like to thank my advisor for the 2011-2012 academic year, Dr. Candace Grand Pre, and my advisors for the 2010-2011 academic years, Dr. Dorothy Merritts and Dr. Robert Walter, for their guidance, mentorship, and commitment to helping me in and out of the classroom. I would also like to thank students Laura Kratz, Amalia Handler, Steven Becker, Conor Neal, Ali Neugebauer, Erik Olsen, Peter Rippenberger, Elvis Andino, Danielle Verna, James Jolles, Jordan Appleyard, Julia Signorella, Kelly Marchisio, James Tracy, Andrew Geltman and Sara Miller for their help with anything from particle size analysis to companionship on otherwise lonely trips to Big Spring Run. Thanks to Prof. Merritts, Prof. Richter, and Drew Altland for serving on my defense committee. Finally, many thanks to Cheryl Shenk for her excellent photographic skills and Mike Rahnis for help with all technical matters.

9. Figures

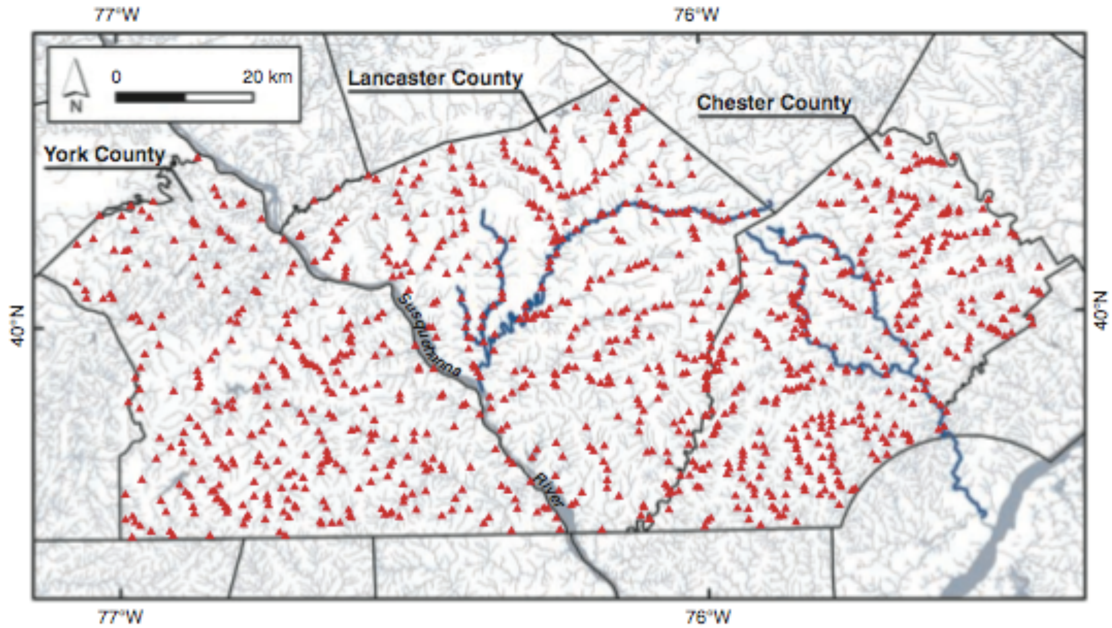

Figure 1. Dams in York, Lancaster, Chester Counties. These counties make up only a small portion of the Chesapeake Bay Watershed. Dams are pervasive in similar quantities throughout the rest of the watershed. There are roughly 400 dams in each county (Walter and Merritts, 2008).

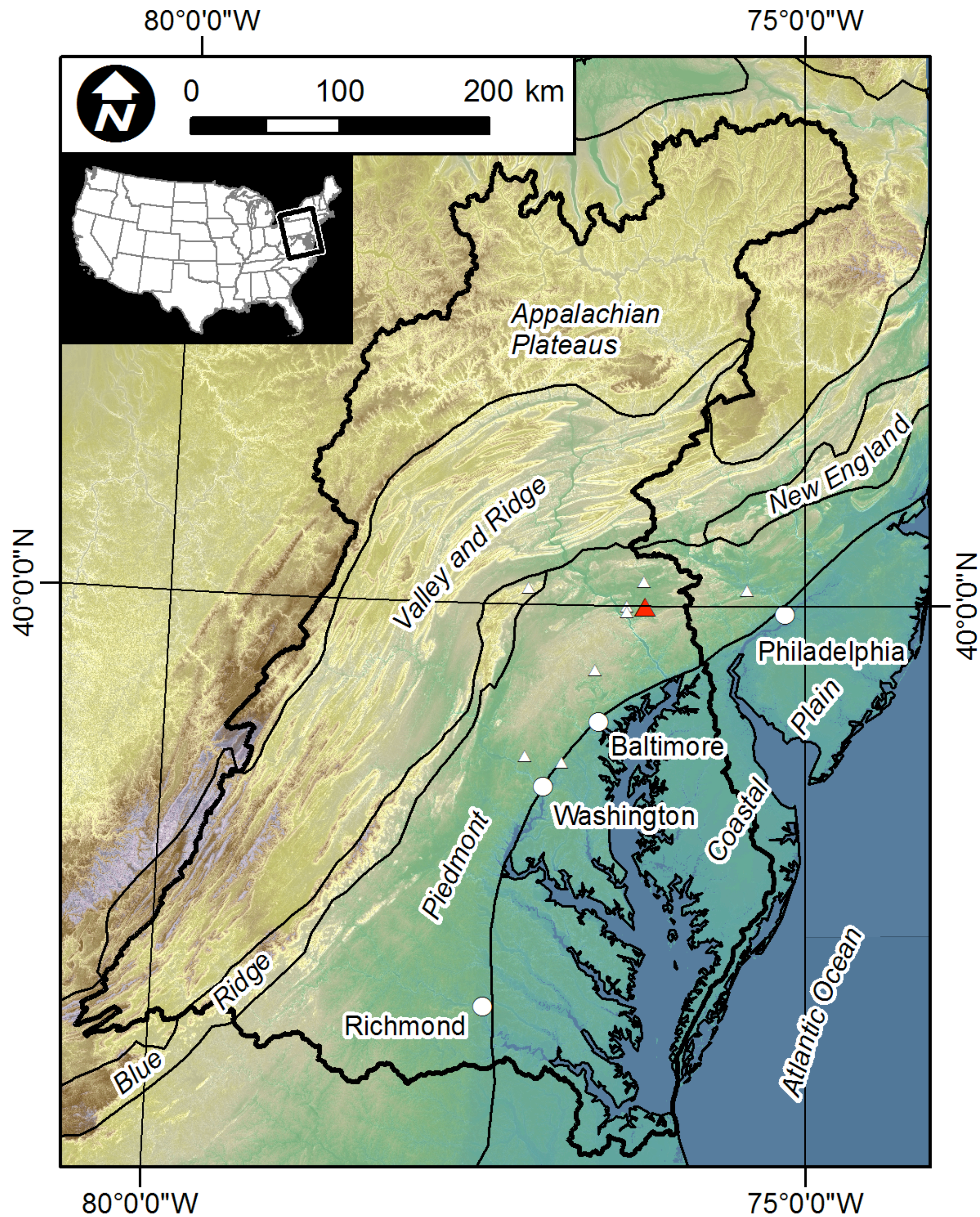

Figure 2: Big Spring Run's location (red triangle) within the Chesapeake Bay Watershed. White triangles refer to sites with similar anthropogenic modifications (image courtesy of Dorothy Merritts).

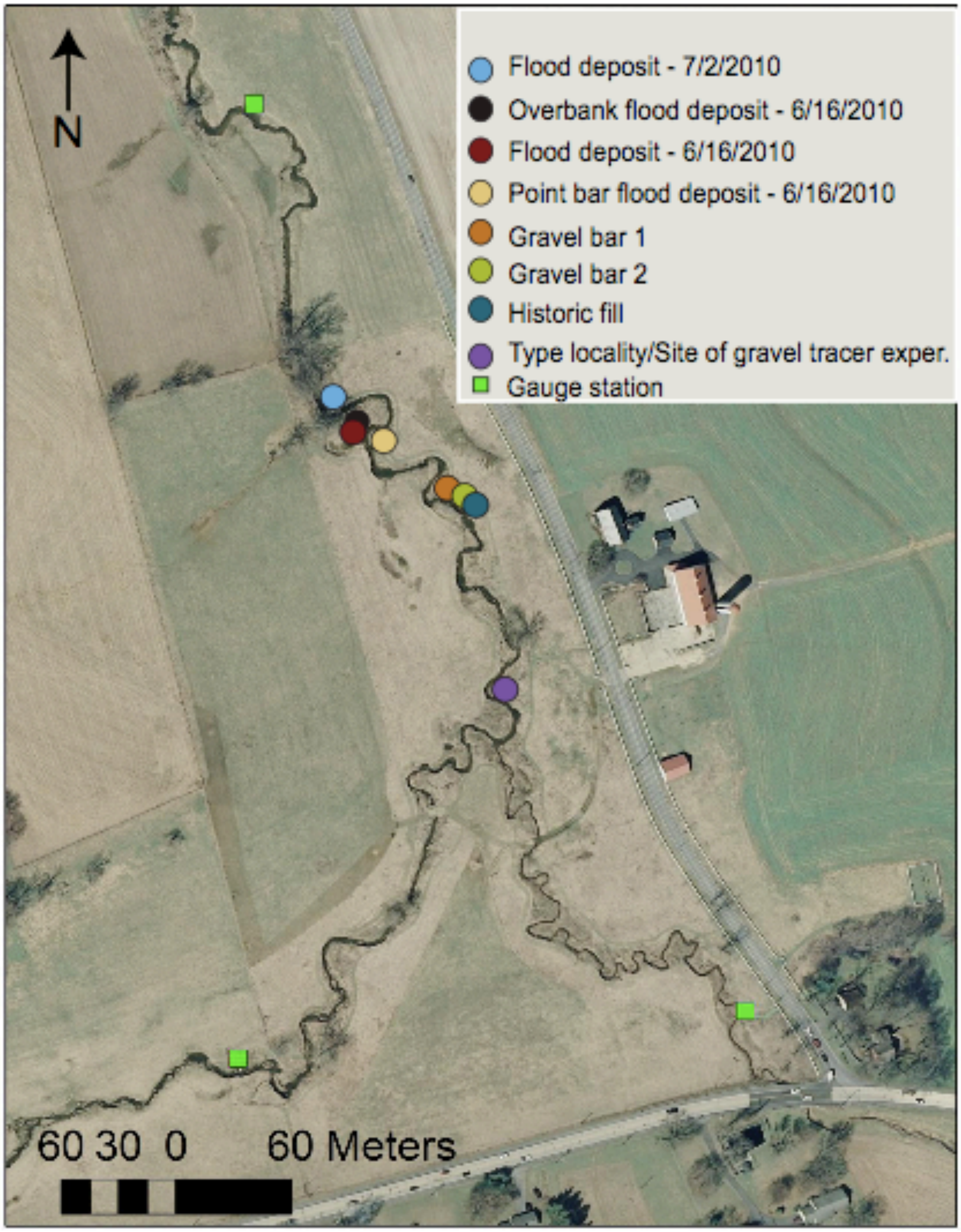

Figure 3: Site Map. USGS gage stations, shown as green squares, were used to measure water height, discharge, and turbidity. Colored circles indicate sample sites. The purple circle, labeled "Type Locality" was the site of tracer gravel experiments.

Figure 4: Modern Analog of BSR during the Pleistocene, before wetlands accumulated in the valley bottoms. Image taken in a valley bottom in Alaska. The angular gravel transported downslope as colluvium by mass wasting processes like gelifluction and solifluction makes up much of the active bed of BSR. Image courtesy of Ellen Wohl.

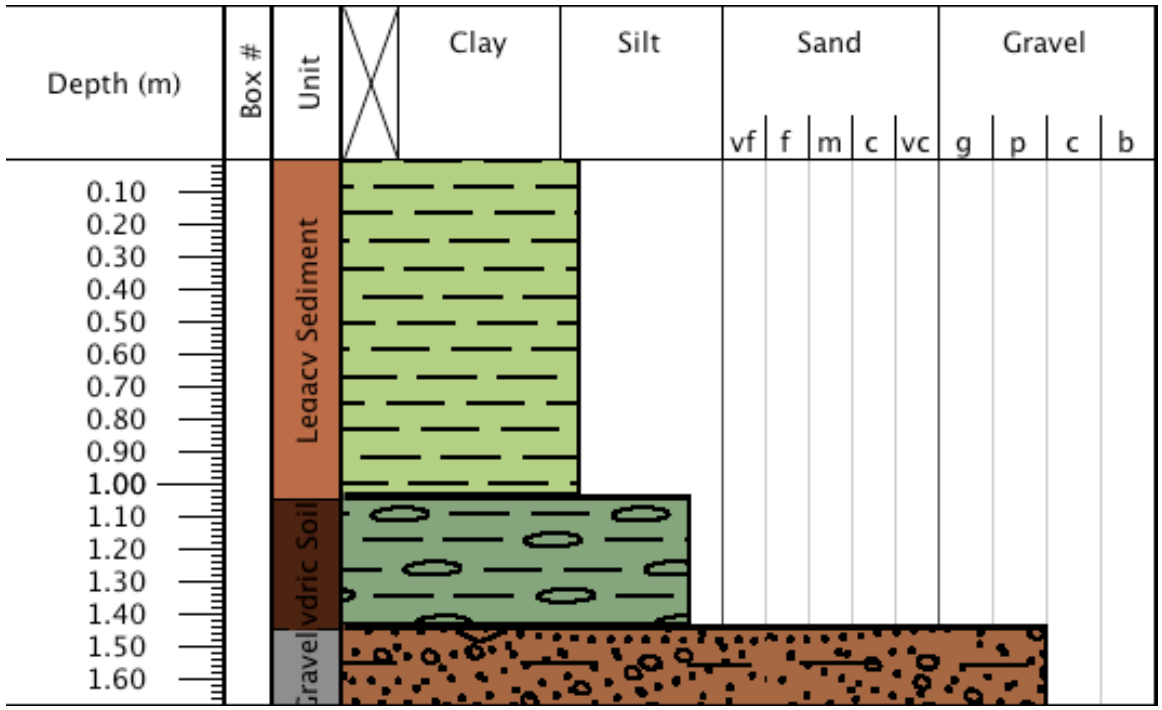

Figure 5: Stratigraphic Column of the stream banks at BSR. The gravel bed of the stream is much coarser than any other unit. The “Hydric Soil” layer is associated with the wet meadow paleoenvironment that was in place at BSR before settlement. The “Legacy Sediment” layer is extremely fine and is the result of sediment that was built up behind dams before flooding the valley bottom during dam breaches.

Figure 6: BSR Streambank. Note the distinct stratigraphic units of 1) Pleistocene Gravel; 2) Buried Hydric soil, wet meadow; 3) Legacy sediment. Units are described from bottom to top of sequence.

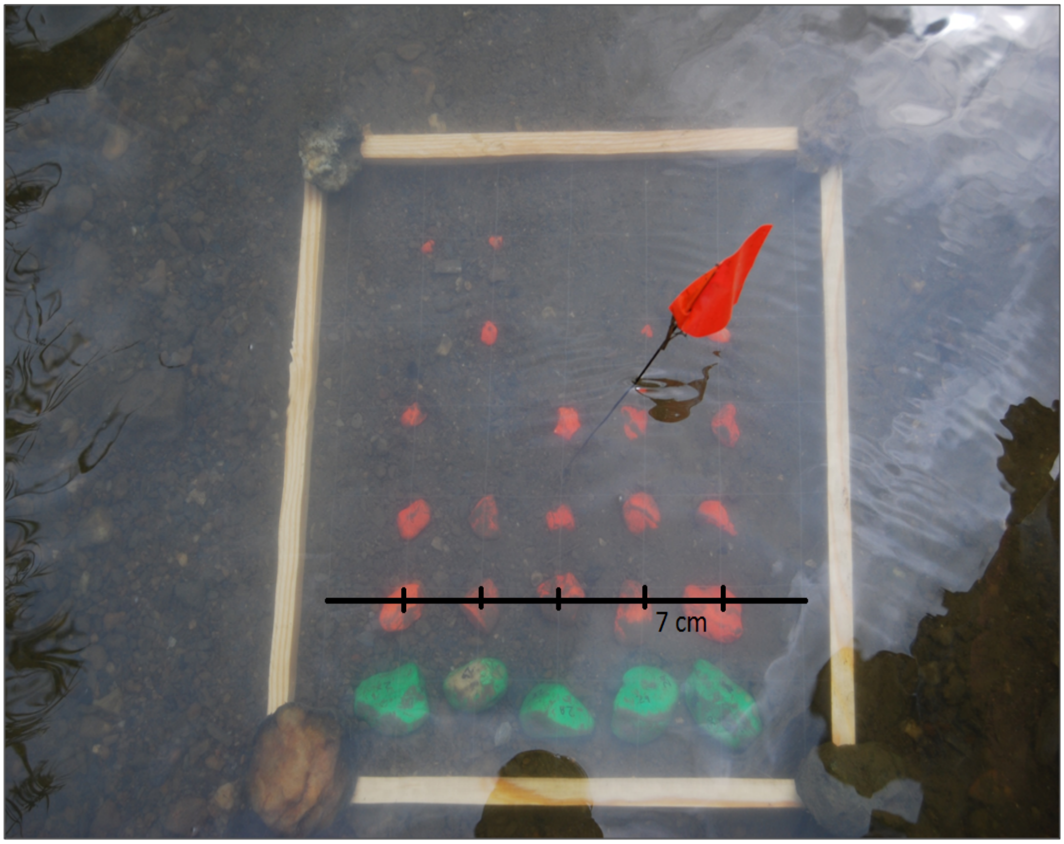

Figure 7: Wooden grid apparatus used to quantify magnitude and direction of gravel transport from June 16th, 2010 – March 6th 2011.

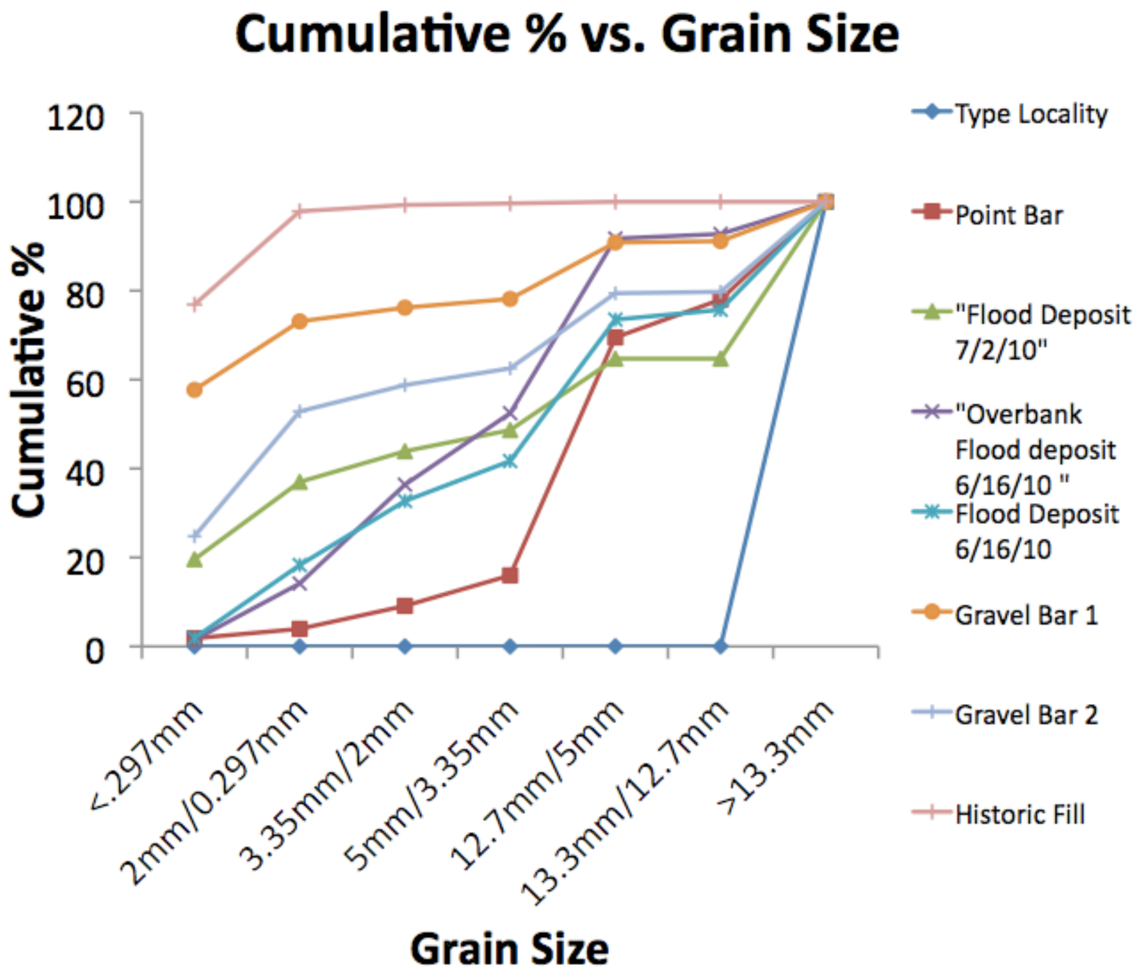

Figure 8. Cumulative % Finer vs. Grain Size graph. This plot characterizes the grain sizes of different sample sites. Note that the "Historic Fill" sample is composed almost entirely of silt and clay. Data for the "Type Locality" sample, the site of the gravel tracer experiment, was taken using the Wolman Pebble Count and shows that the active bed is predominanty composed of coarse gravel. See Figure 3 for site locations.

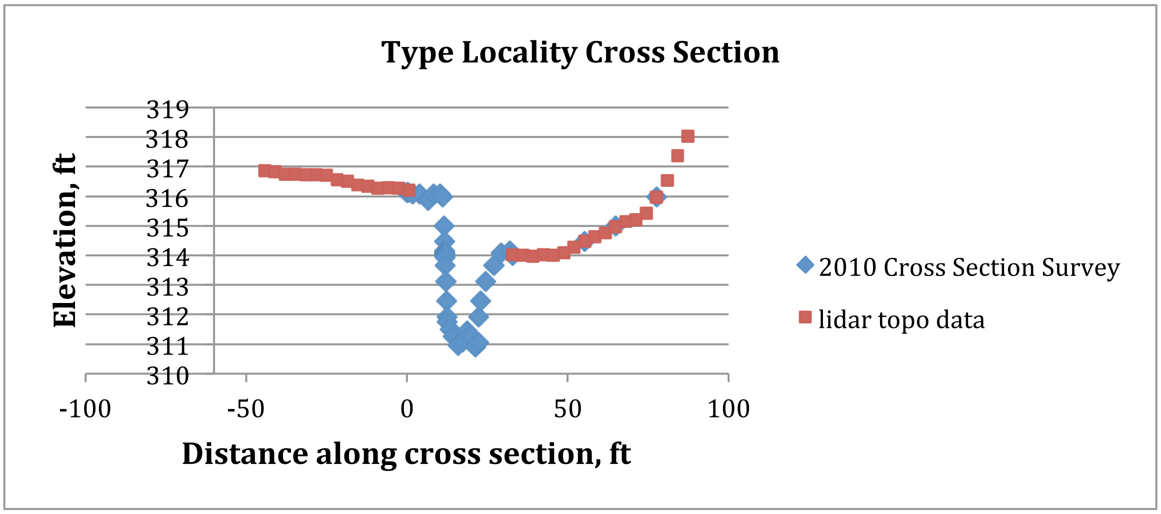

Figure 9: Cross section of Type Locality using 2010 cross section survey as well as LIDAR topographical data. This cross section was used to calculate hydraulic radius during various storm events.

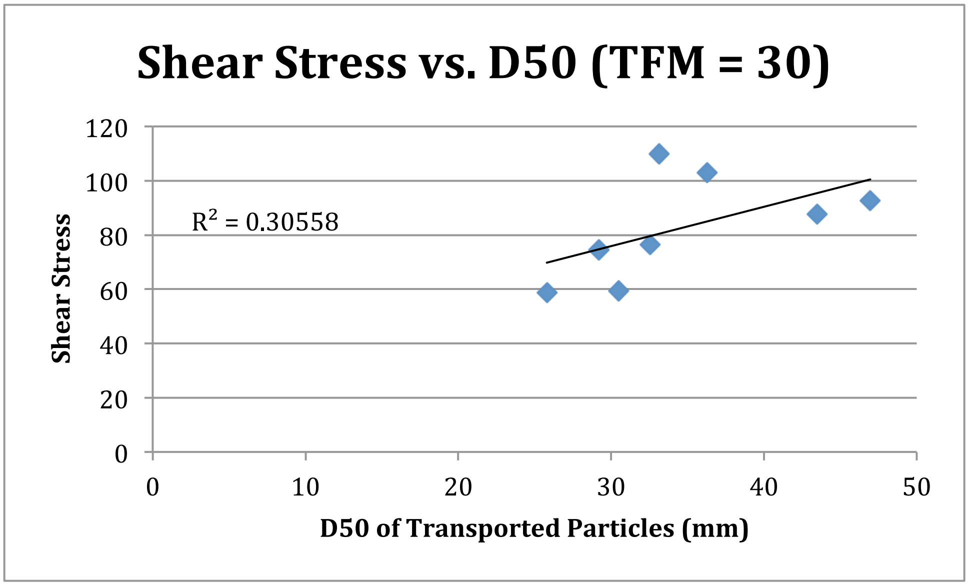

Figure 10: Shear stress vs. D_{50} of transported particles ("Movement" = 30 cm). A positive and causal relationship can be seen when examining shear stresses and D_{50} of particles transported. Higher shear stresses should be able to transport larger particles. Low R^2 values can be attributed to small sample size and the generally stochastic nature of fluvial sediment transport.

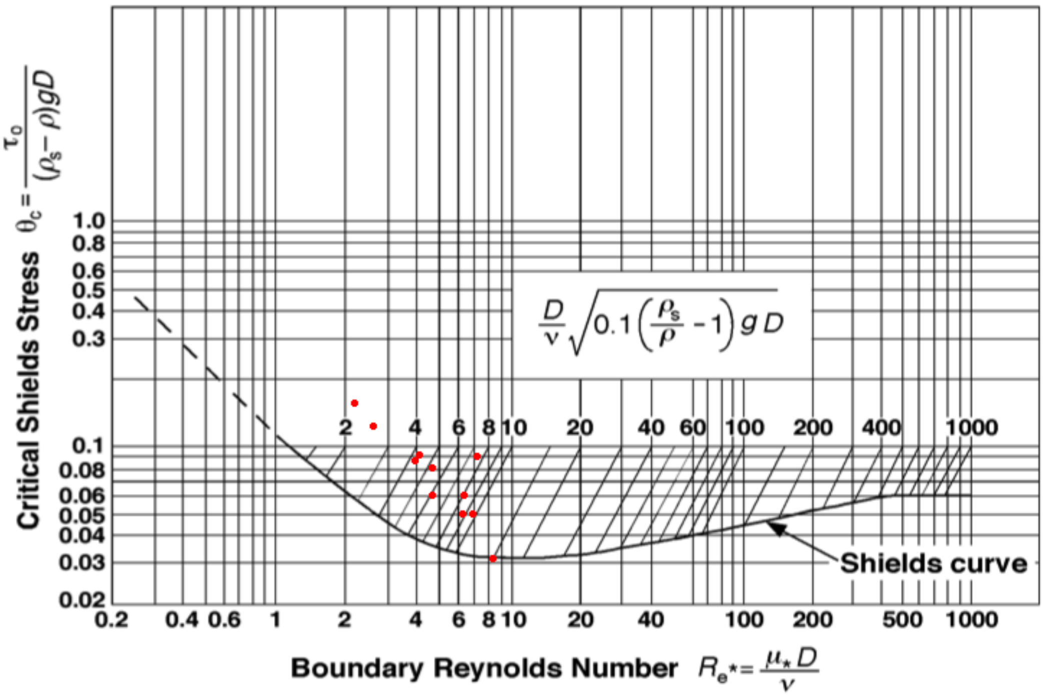

Figure 11: Data points for each high flow event during the study period were plotted on this Shields Curve (Shields, 1936). Each red dot represents a high flow event. Note that each point falls within zone of transport, which confirms that the clasts measured in this study were capable of active transport.

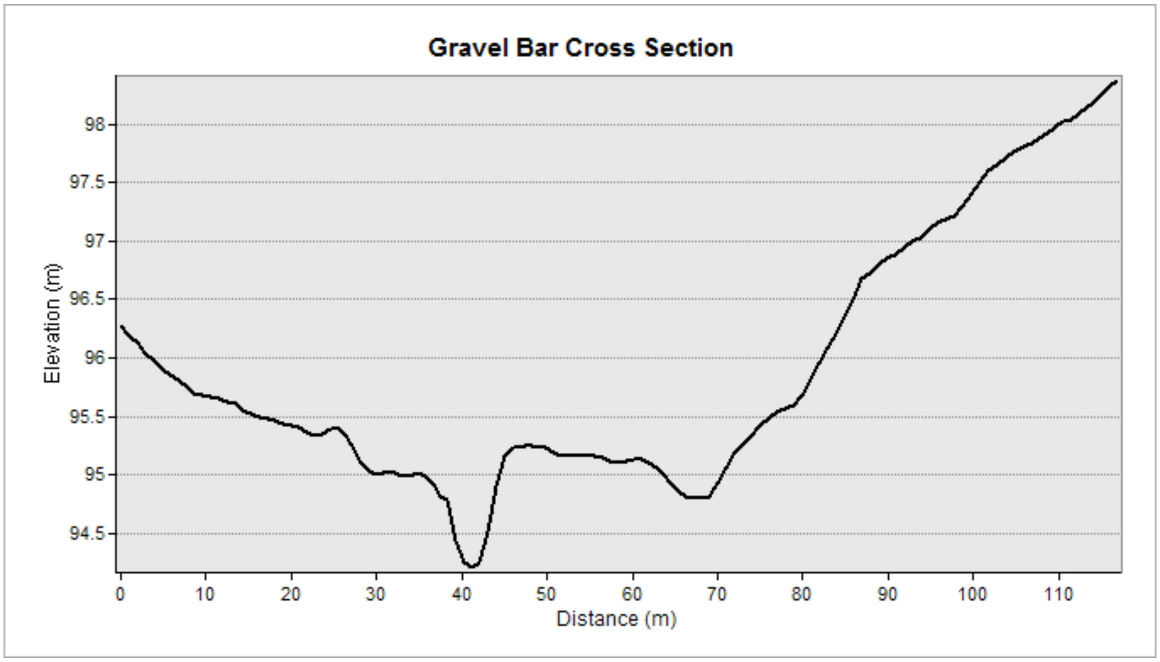

Figure 12: Cross Sections for “Gravel Bar 1”, “Gravel Bar 2”, and “Point Bar” samples shown in Figure 3.

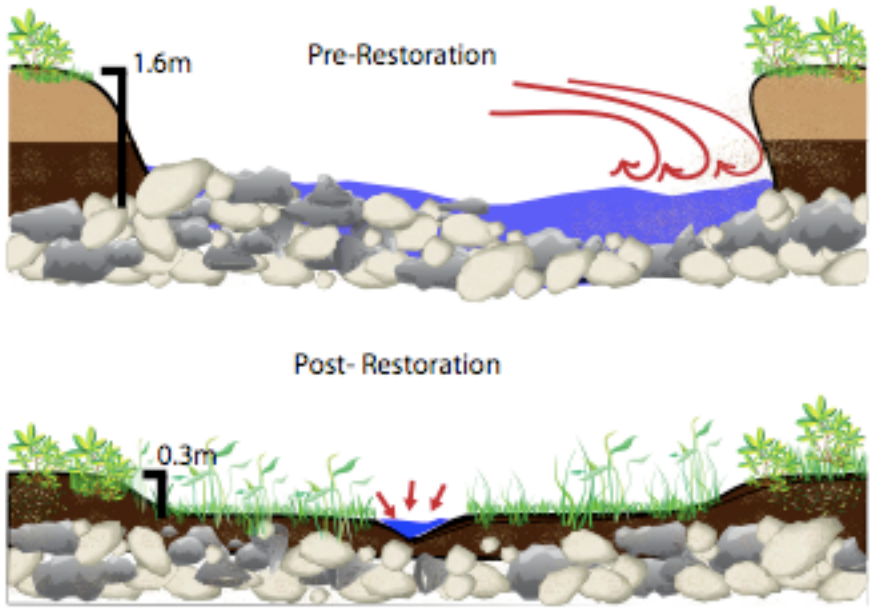

Figure 13: Pre- and Post-restoration conditions at BSR. It is important to note the decreased bank heights, wide floodplain, and flow vectors associated with post-restoration figures. This contrasts with the pre- restoration conditions that feature higher banks, increased erosion of banks, and larger flow vectors that increase the potential for gravel transport (illustration by Grand Pre, unpublished).

10. Table

Date of Event	Water Depth, m	Hydraulic Radius (R), m	D50, mm	Shear Stress from Depth (Pa)	Shear Stress from R (Pa)	Shield's Parameter	Shear Velocity, u_*, m/sec	Boundary Reynolds No.
6/24/2010	0.79	0.47	23.35	53.97	32.22	0.09	0.18	4.19
6/27/2010	0.80	0.47	21.89	54.63	32.29	0.09	0.18	3.93
6/17/2010	0.83	0.47	12.60	56.62	32.41	0.16	0.18	2.27
7/12/2010	0.85	0.47	14.63	58.44	32.36	0.14	0.18	2.63
3/16/2011	0.85	0.47	25.79	58.60	32.35	0.08	0.18	4.64
4/8/2011	0.86	0.47	34.84	59.27	32.30	0.06	0.18	6.26
4/5/2011	0.88	0.47	38.58	60.43	32.15	0.05	0.18	6.92
3/6/2011	1.09	0.39	29.20	74.50	26.99	0.06	0.16	4.80
3/11/2011	1.11	0.38	52.28	76.32	26.06	0.03	0.16	8.44
4/16/2011	1.28	0.31	23.48	87.74	21.56	0.06	0.15	3.45
4/28/2011	1.35	0.32	43.66	92.70	21.63	0.03	0.15	6.42
10/1/2010	1.50	0.44	36.27	102.97	30.31	0.05	0.17	6.31
7/26/2010	1.60	0.67	33.12	109.76	45.86	0.09	0.21	7.09

Table 1: The table depicts flow events, water depth, hydraulic radius (R), D_{50} of transported clasts, shear stresses calculated using water depth, shear stresses calculated using hydraulic radius, Shields parameter, shear velocity and boundary Reynolds number at BSR from June 2010 to April 2011. Events are arranged from lowest to highest water depths. Shear stress was calculated from depth using the equation Tb = pghS where Tb = shear stress, p = density, g = acceleration due to gravity, h = water height, and S = slope. Shear stress was calculated from hydraulic radius (R), using the equation Tb = pgRS, where p = density, g = acceleration due to gravity, R = hydraulic radius, and S = slope.

11. References

Bernhardt ES, Palmer MA, Allan JD, Alexander G, Barnas K, Brooks S, et al. (2005) Synthesizing USA river restoration efforts. Science 308: 636–637.

Blackmer, Gale C. 2007. Bedrock Geologi Map of the Quarryville and Conestoga Quadrangles, Lancaster County, Pennsylvania. Open File Report. 4th Series. Harrisburg, PA: Pennsylvania geological Survey. http://www.dcnr.state.pa.us/topogeo/openfile/conquarry.pdf.

Fraley, L. 2006. Interaction between channel morphology and spatial patterns of sediment storage and remobilization in Valley Creek, Valley Forge National Historical Park. Master'sThesis, University of Maryland Baltimore Campus.

Galeone, Daniel G.; Low, Dennis J.; Brightbill, Robin A., 2006, FS 2006-3112: Effects of streambank fencing of near-stream pasture land on a small watershed in Lancaster County, Pennsylvania. 1993-2001. Scientific Investigators Report 2006-5141. Reston, VA; Denver, CO: U.S. Dept of the Interior, U.S. Geological Survey

Gee, G.W., and J.W. Bauder. 1986. Particle-size analysis. p. 383–411. In A. Klute (ed.) Methods of soil analysis. Part 1. 2nd ed. Agron. Monog. 9. ASA and SSSA, Madison, WI.

Hilgartner, William B., and Grace S. Brush. "Prehistoric habitat stability and post-settlement habitat change in a Chesapeake Bay freshwater tidal wetland, USA." The Holocene 16, no. 4 (May 1, 2006): 479-494.

Jerolmack, D. J., Reitz, M. D., and Martin, R. L., 2011, Sorting out abrasion in a gypsum dune field, Journal of Geophysical Research, Volume 116, AGU.

Langland, M.J., Phillips, S.W., Raffensperger, J.P., and Moyer, D.L., 2005, Changes in streamflow and water quality in selected nontidal sites in the Chesapeake Bay Basin, 1985-2003: U.S. Geological Survey Scientific Investigations Report 2004-5259, 50 p.

Leopold, L. B., M. Wolman, and J. Miller,1964. Fluvial Processes in Geomorphology .W. H. Freeman, San Francisco, CA

Leopold, Luna B., and Wolman, M.G., 1956, Floods in Relation to the River Channel, in Union Geod. et Geophysics International, Association d'Hydrologie (Symposium in Dijon), Publication no.42, p.85-98.

Merritts, D., Walter, R., Rahnis, M., Hartranft, J., Cox, S., Gellis, A., Potter, N., Hilgartner, W., Langland, M., Manion, L., Lippincott, C., Siddiqui, S., Rehman, Z., Scheid, C., Kratz, L., Shilling, A., Jenschke, M., Datin, K., Cranmer, E., Reed, A., Matuszewski, D., Voli, M., Ohlson, E., Neugebauer, A., Ahamed, A., Neal, C., Winter, A., and Becker, S., 2011, Anthropocene streams and base-level controls from historic dams in the unglaciated mid-Atlantic region, USA: Philosophical Transactions of the Royal Society A: Mathematical, Physical and Engineering Sciences, v. 369, no. 1938, p. 976-1009.

Montgomery, D. R., 2008, Dreams of natural streams: Science, v. 319, no. 5861, p. 291-292.

Neugebauer, Ali. “Paleoecological Reconstruction of Big Spring Run, Lancaster, PA.” Undergraduate Honors Thesis. Franklin and Marshall College, May 2011.

Parker, G., 1978, Self-formed straight rivers with equilibrium banks and mobile bed. Part 2. The gravel river. : Journal of Fluid Mechanics v. 89, p. 127-146.

Phillips, S.W., Barlow, R.A., Brakebill, J.W., Bratton, J.F., Blazer, V.S., Bohlke, J.F., Bricker, O.P., Colman, S.M., Cronin, T.M., Hupp, C.R., Keough, J.R., Landwehr, J.M., Langland, M.J., Newell, W.L., Perry, M.C., Phillips, S.W., Preston, S.D., Rybicki, N.B., Simon, N.S., Willard, D.A. 2002. The U.S. Geological Survey and the Chesapeake Bay - The role of science in environmental restoration: U.S. Geological Survey Circular 1220. (online report)

Phillips, S.W. 2001, The Impact of Sediment on the Chesapeake Bay and its Watershed. U.S. Department of the Interior, U.S. Geological Survey. Available at: http://chesapeake.usgs.gov/SedimentBay605.pdf

Phillips, S. W. ed. 2002 The U.S. Geological Survey and the Chesapeake Bay—The role of science in environmental restoration. Reston, VA: U.S. Department of the Interior, U.S. Geological Survey. Available at: http://pubs.usgs.gov/circ/c1220

Senus, M.P., Langland, M.J., and Moyer, D.L., 2005, Nutrient and sediment concentrations, loads, and trends for four nontidal tributaries in the Chesapeake Bay watershed, 1997-2001: U.S. Geological Survey Scientific Investigations Report 2004-5125, 33 p.

Shields, A. (1936), Anwendung der A¨ hnlichkeitsmechanik und der Turbulenzforschung auf die Geschiebebewegung, Mitt. Preuss. Versuchsanst. Wasser., 26.

Shilling, Andrea. “Rates and processes of stream bank erosion to suspend sediment load, Big Spring Run, PA.” Undergraduate Honors Thesis. Franklin and Marshall College, May 2010.

Smith, V.H.; G.D. Tilman, and J.C. Nekola (1999). "Eutrophication: impacts of excess nutrient inputs on freshwater, marine, and terrestrial ecosystems". Environmental Pollution 100 (1-3): 179–196. doi:10.1016/S0269-7491(99)00091-3. PMID 15093117.

Snyder, N. P., Castele, M. R., and Wright, J. R., 2008, Bedload entrainment in low-gradient paraglacial coastal rivers of Maine, U.S.A.: Implications for habitat restoration: Geomorphology, v. 103, no. 3, p. 430-446.

Voli, Mark, Dorothy Merritts, Robert Walter, Erik Ohlson, Katherine Datin, Michael Rahnis, Laura Kratz, Wanlin Deng, William Hilgartner, and Jeffrey Hartranft. “Preliminary Reconstruction of a Pre-European Settlement

Valley Bottom Wetland, Southeastern Pennsylvania." Water Resources Impact 11, no. 5 (September 2009): 11-12.

Voli, Mark. "Reconstructing pre-European settlement paleo-environments in Piedmont valley bottoms." Senior Thesis. Unpublished. April 2009.

Walter, R. C., and Merritts, D. J., 2008, Natural streams and the legacy of water-powered mills: Science, v. 319, no. 5861, p. 299-304.

Wiberg, P. L., and Smith, J. D., 1987, Calculations of the critical shear stress for motion of uniform and heterogeneous sediments Water Resources Research, v. 23, p. 1471-1480.

APPENDIX 1: Threshold for Movement Plots

These plots are attached in order to characterize the problem for what is considered to be "incipient motion". Different thresholds ascribed to be "incipient motion" yield different R^2 values. It is important to note how these values change as different thresholds for "incipient motion" are used. Furthermore, R^2 values change when using the D_{84} of transported particles as opposed to the D_{50} of transported particles. Both the D_{50} and the D_{84} were used in this appendix in order to determine if the size percentile of transported clasts had an impact on R^2 values. It might benefit further studies if the term "incipient motion" was ascribed a standardized, more specific definition. Note that the acronym TFM means "threshold for movement", and characterizes what we considered to be "incipient motion" in each plot.

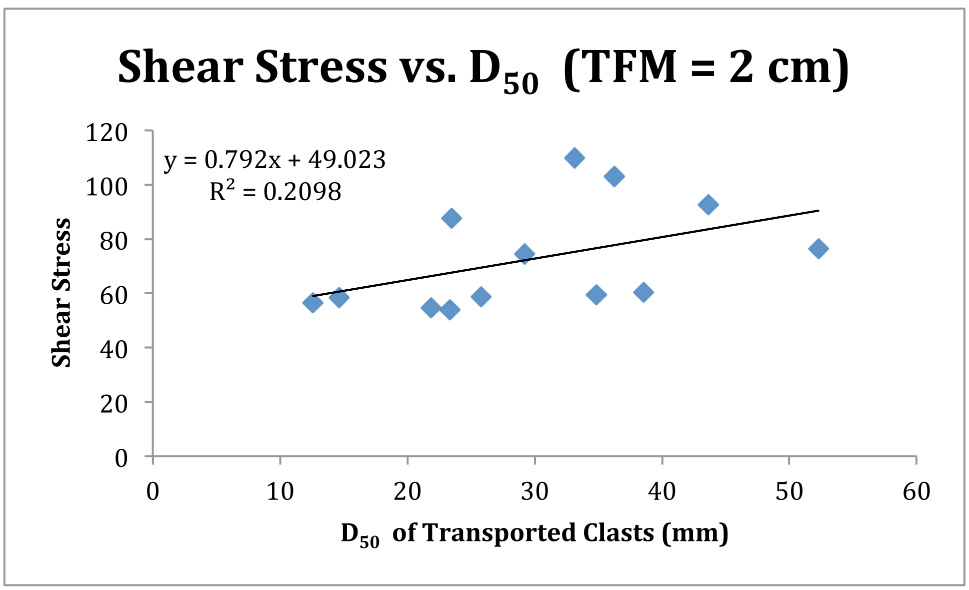

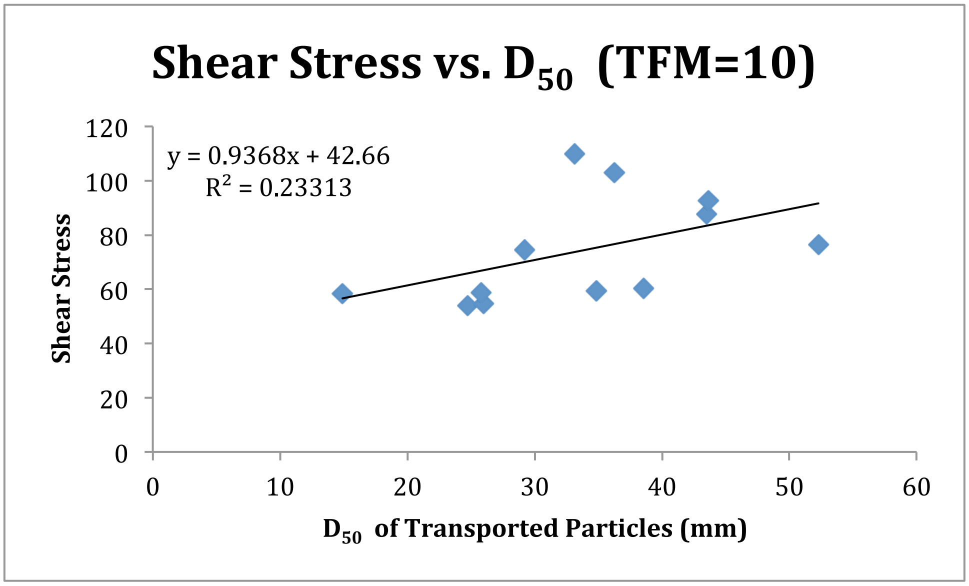
Shear Stress vs. D50 (TFM=10)
y = 0.9368x + 42.66
R² = 0.23313
Shear Stress
0
20
40
60
80
100
120
0
10
20
30
40
50
60
D50 of Transported Particles (mm)

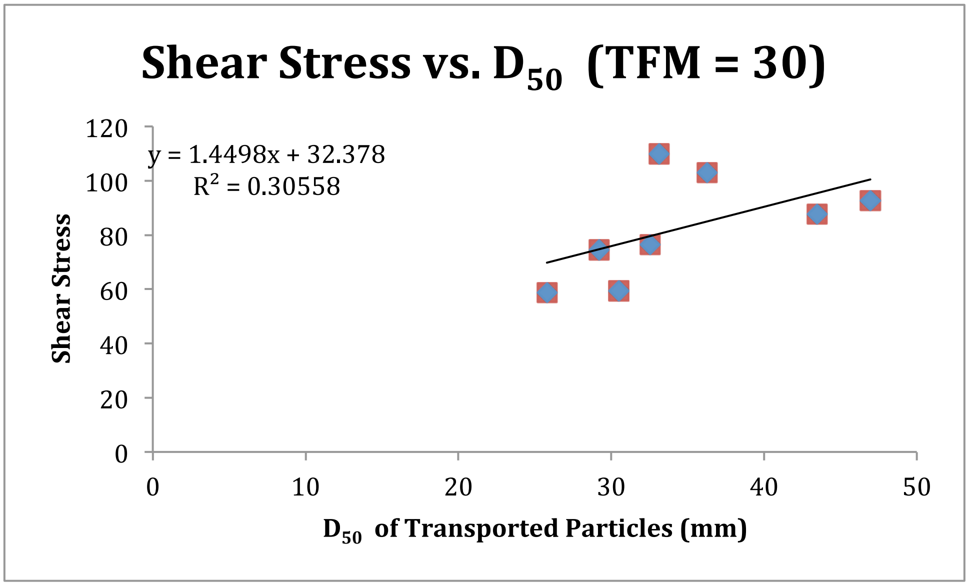
Shear Stress vs. D50 (TFM = 30)
y = 1.4498x + 32.378
R2 = 0.30558
Shear Stress
D50 of Transported Particles (mm)
120
100
80
60
40
20
0
0
10
20
30
40
50

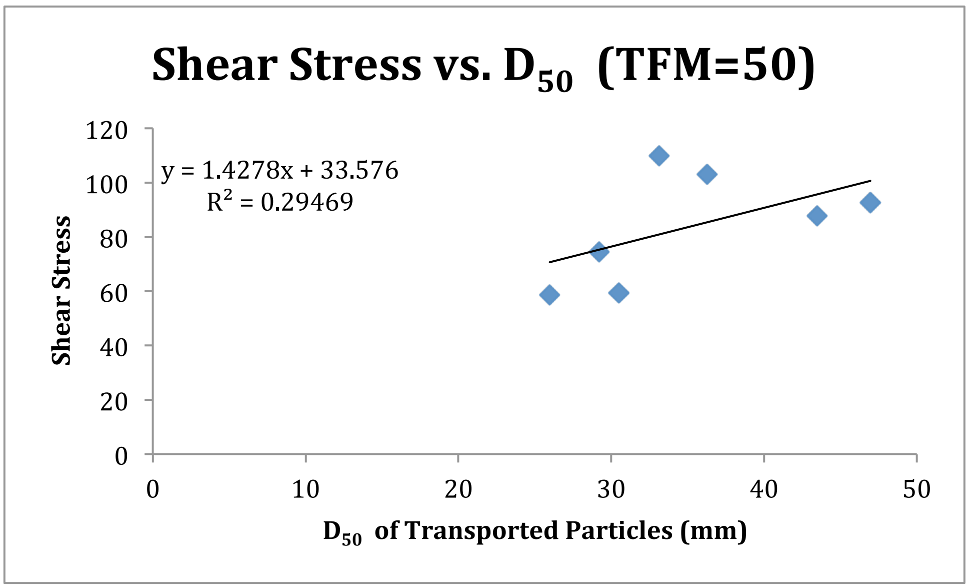
Shear Stress vs. D50 (TFM=50)
y = 1.4278x + 33.576
R2 = 0.29469
Shear Stress
D50 of Transported Particles (mm)
120
100
80
60
40
20
0
0
10
20
30
40
50

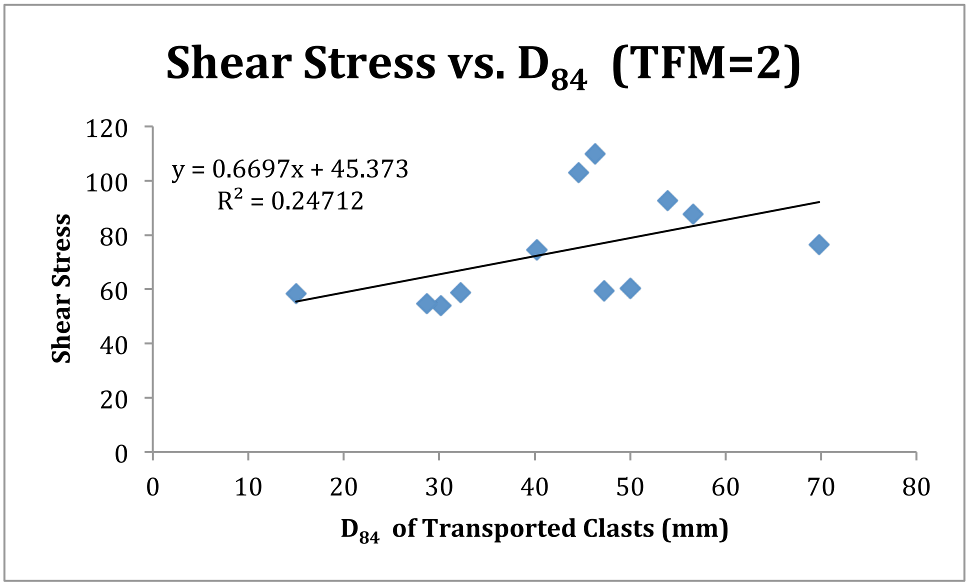
Shear Stress vs. D84 (TFM=2)
y = 0.6697x + 45.373
R2 = 0.24712
Shear Stress
120
100
80
60
40
20
0
0
10
20
30
40
50
60
70
80
D84 of Transported Clasts (mm)

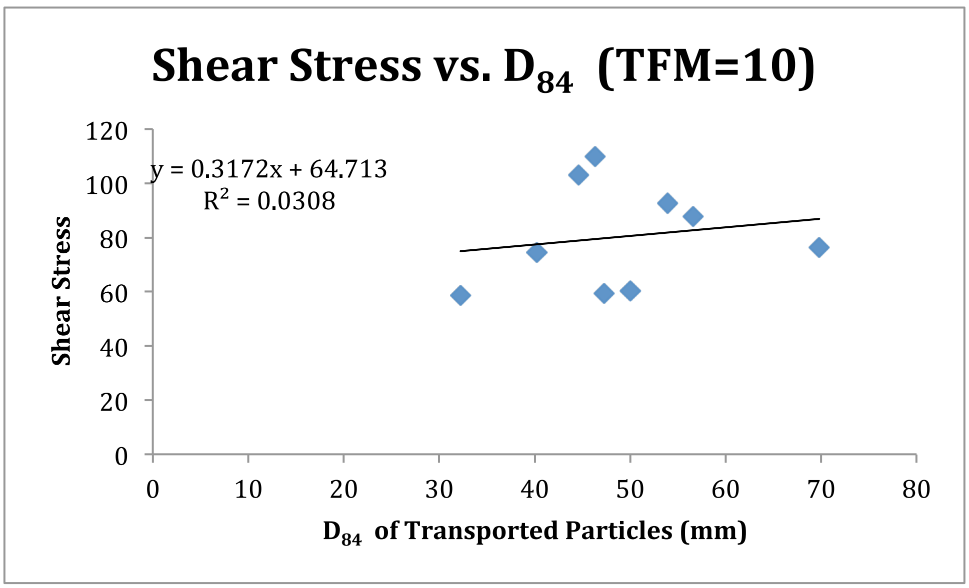
Shear Stress vs. D84 (TFM=10)
y = 0.3172x + 64.713
R2 = 0.0308
Shear Stress
120
100
80
60
40
20
0
0
10
20
30
40
50
60
70
80
D84 of Transported Particles (mm)

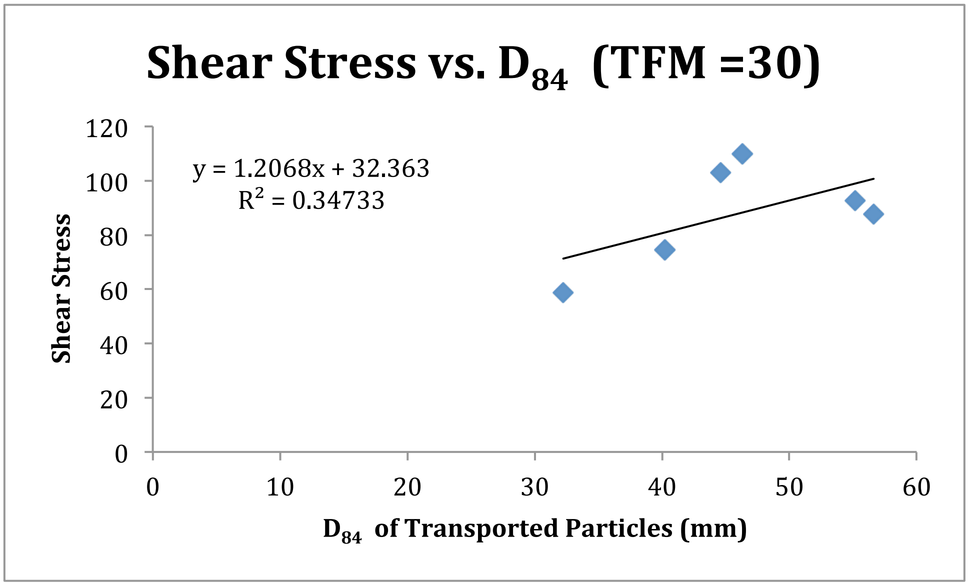
Shear Stress vs. D84 (TFM =30)
y = 1.2068x + 32.363
R2 = 0.34733
Shear Stress
120
100
80
60
40
20
0
0
10
20
30
40
50
60
D84 of Transported Particles (mm)

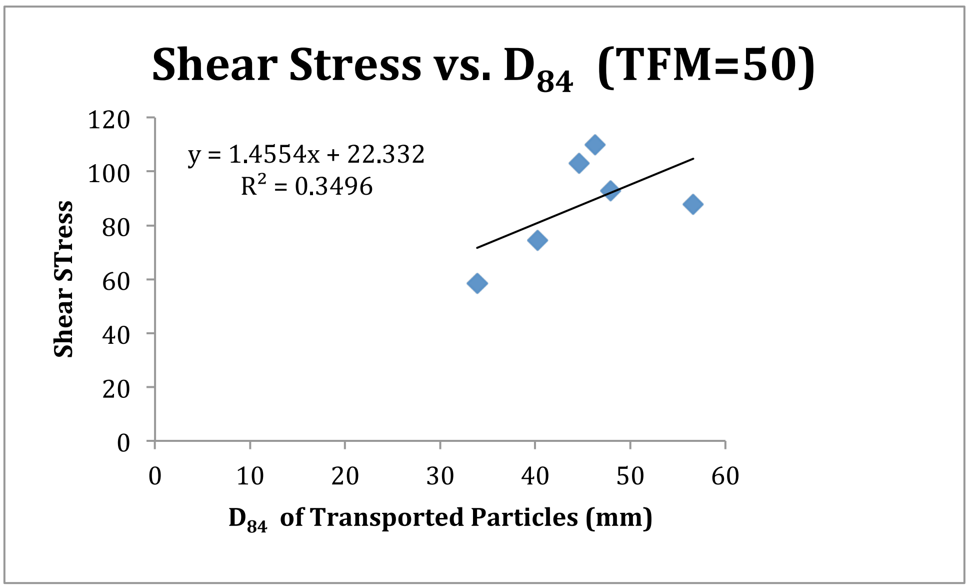
Shear Stress vs. D84 (TFM=50)
y = 1.4554x + 22.332
R2 = 0.3496
Shear STress
120
100
80
60
40
20
0
0
10
20
30
40
50
60
D84 of Transported Particles (mm)